DEUTERANOPIA FIGURES FOR SPATIO-TEMPORAL AND CROSS-SCALE INTERACTIONS IN HYDROCLIMATE VARIABILITY: A CASE-STUDY IN FRANCE

Manuel Fossa[1], Bastien Dieppois[2], Nicolas Massei[1], Matthieu Fournier[1], Benoit Laignel[1], and Jean-Philippe Vidal[3]

[1] Normandie Univ, UNIROUEN, UNICAEN, CNRS, M2C, 76000 Rouen, France
[2] Centre for Agroecology, Water and Resilience (CAWR), Coventry University, Coventry, UK
[3] INRAE, UR Riverly, 5 rue de la Doua, CS 20244, 69625 Villeurbanne Cedex, France

Correspondence: Manuel Fossa (manuel.fossa1@univ-rouen.fr)

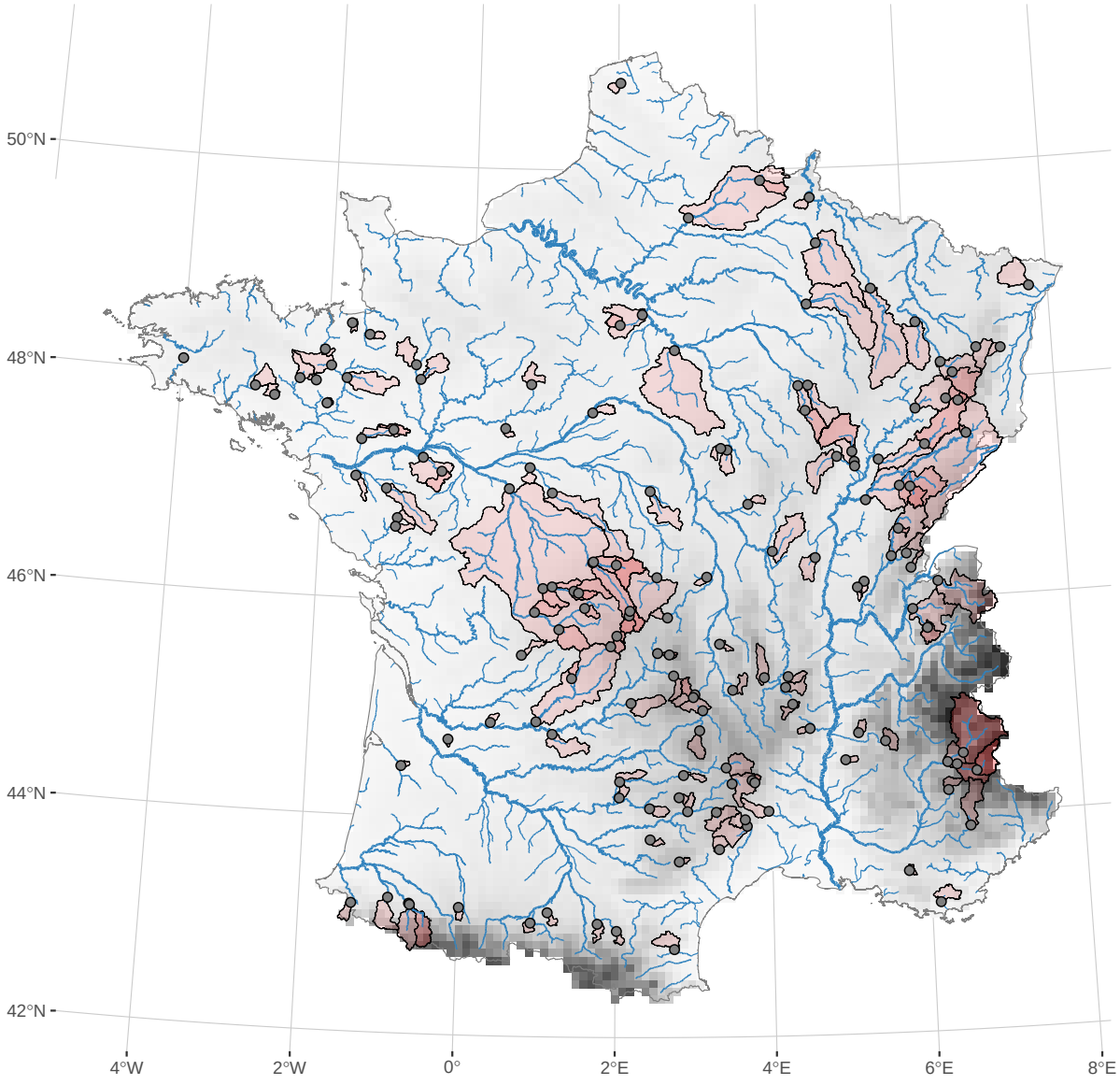

Figure S1. Location of stream gauges (grey dots), corresponding watersheds (pale red, Brigode et al. (2020)), hydrographic network (blue lines, Pella et al. (2012)), and orography in Safran dataset (grey scale, Vidal et al. (2010)).

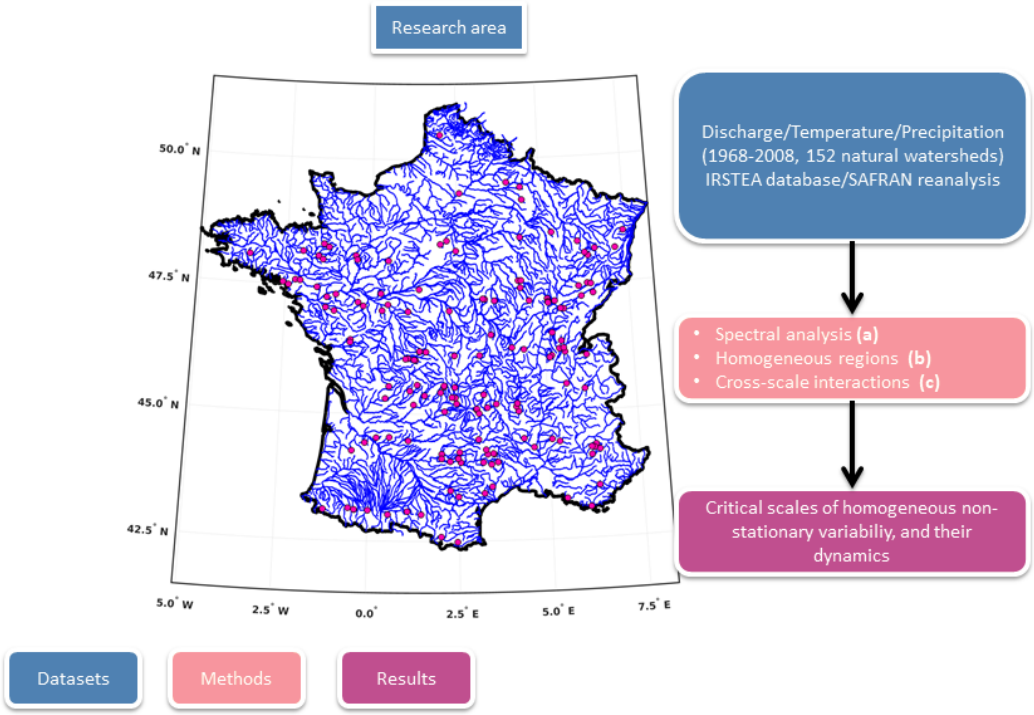

Figure S2. Workflow of this study. (**a**) 152 monthly precipitation, temperature and discharge time series are extracted from IRSTEA's watershed database. The following steps are applied to each variable. (**b**) the continuous wavelet spectrum for each watershed is computed. (**c**) A distance matrix between wavelet spectra is then established; d.) A fuzzy clustering algorithm is used to build a classification map of the watersheds based on their wavelet spectra.

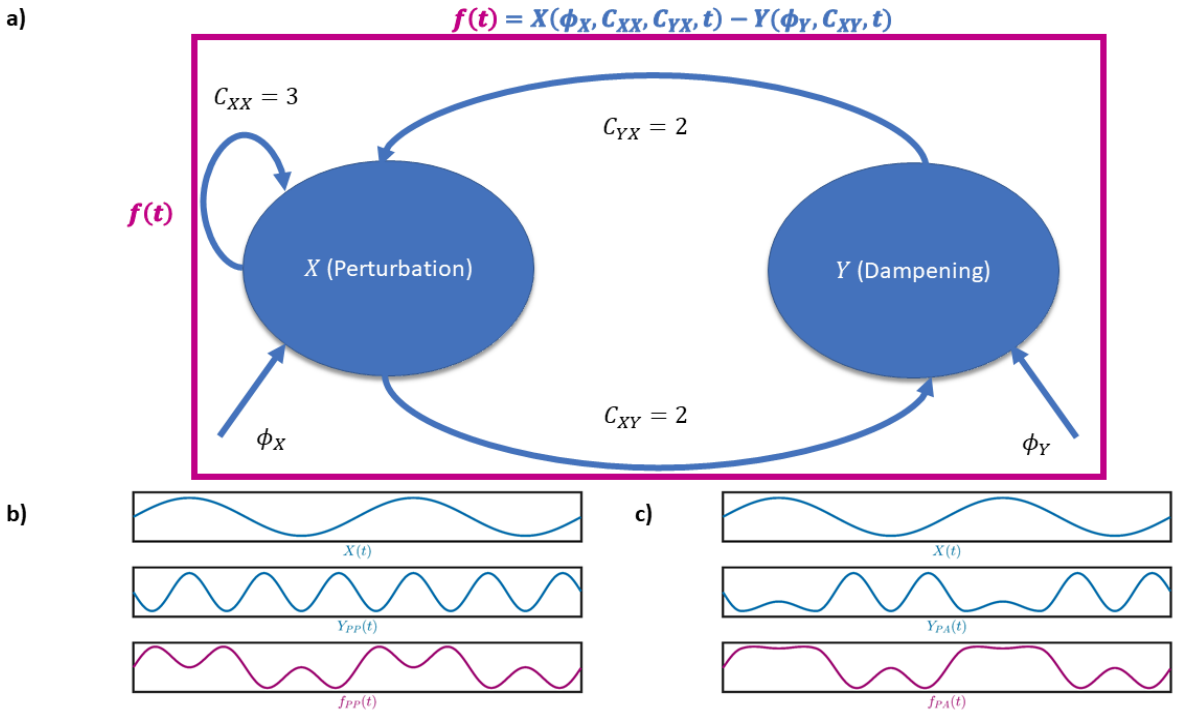

Figure S3. A system with directional cross scale interactions. **a)** A variable $f(t)$ made of two components X and Y, connected through C_{XY} and C_{YX} in a perturbation-dampening scheme so that $f(t) = X(t) - Y(t)$. Both X and Y receive inputs ϕ_X and ϕ_Y, respectively. C_{XX} allows X to grow first. Depending on both inputs and connections, some phase-phase or phase-amplitude interactions between X and Y can occur. **b)** an example of a phase-phase interaction, with every fourth ridge of Y_{PP} coinciding with a ridge of X, with $f_{PP}(t) = X(t) - Y_{PP}(t)$ (top,middle and bottom panels, respectively). **c)** an example of phase-amplitude interaction. X and Y_{PA} only interact when X reaches a ridge, in which case Y_{PA} amplitude if lowered, yielding $f_{PA}(t)$ (Top, middle and bottom panels, respectively). (adapted from Onslow et al. (2014))

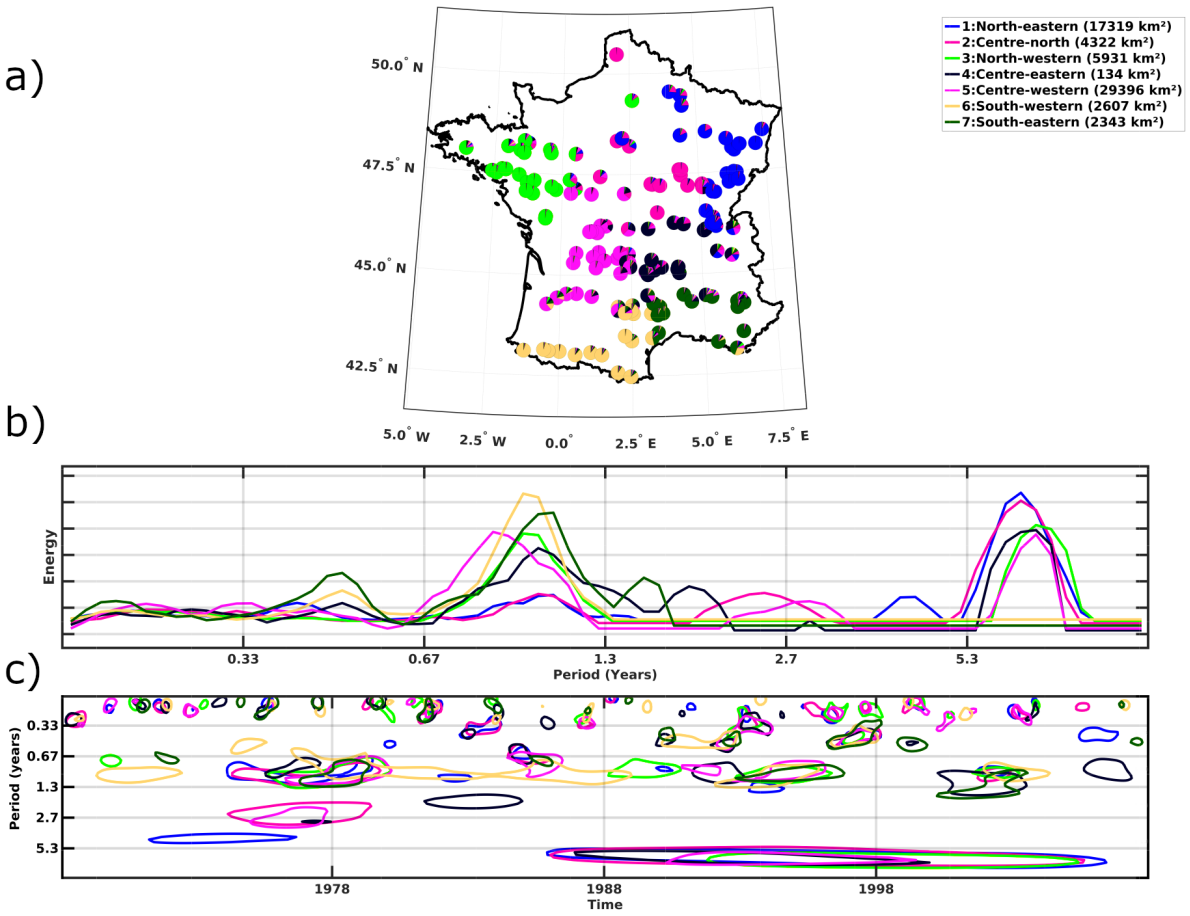

Figure S4. Clustering of precipitation time-frequency variability in France. (**a**) Classification map of the watersheds. Pie charts slices show the three highest probability memberships. Pie charts denote fuzzy clustering memberships. (**b**) Global wavelet spectra for each cluster (95% significance level against red noise). (**c**) Statistically significant wavelet spectra for each cluster.

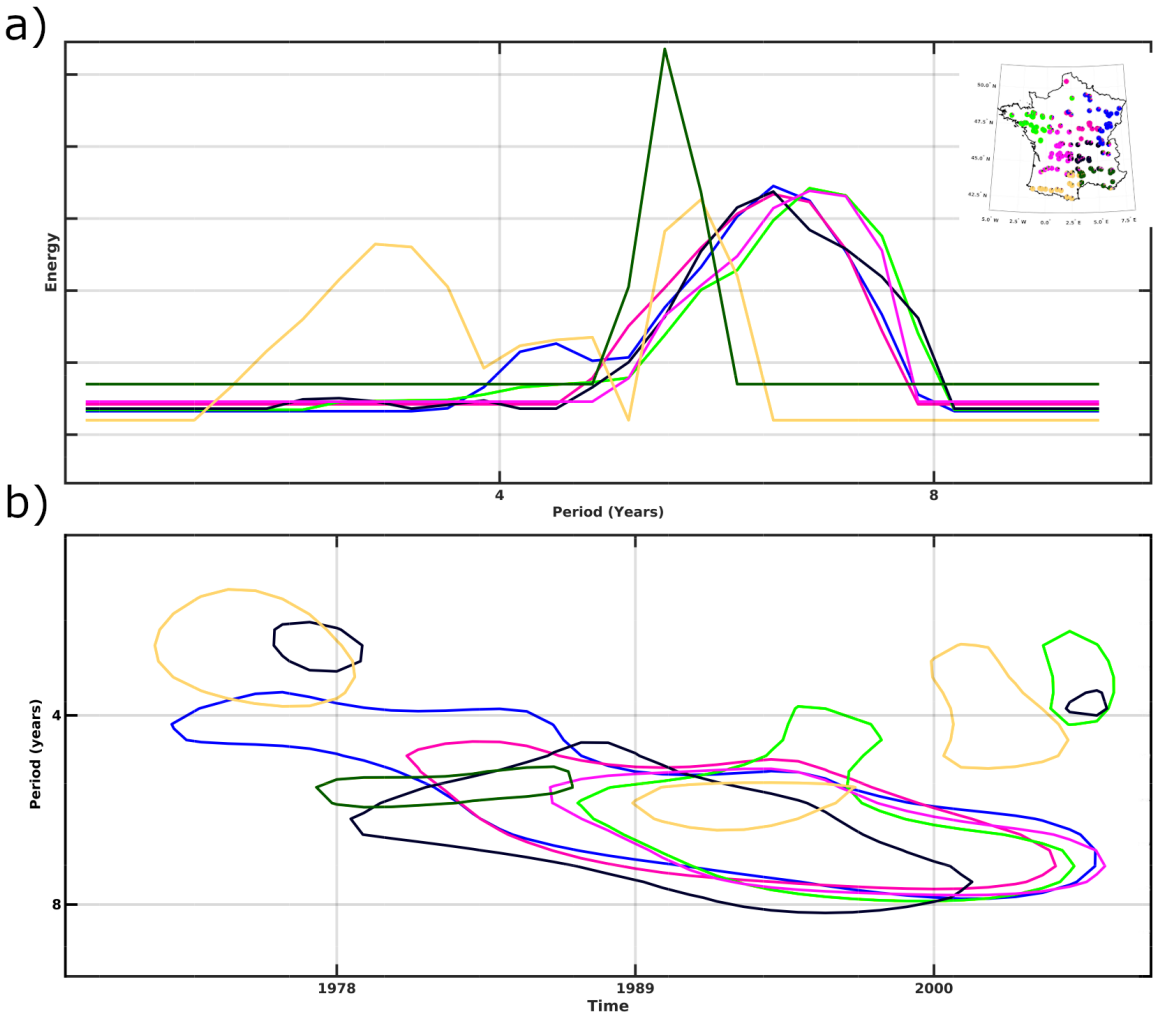

Figure S5. Inter-annual precipitation time-frequency variability in France. (**a**) Global wavelet spectra for each cluster. (**b**) Statistically significant (95% significance level) wavelet spectra for each cluster.

a)

b)

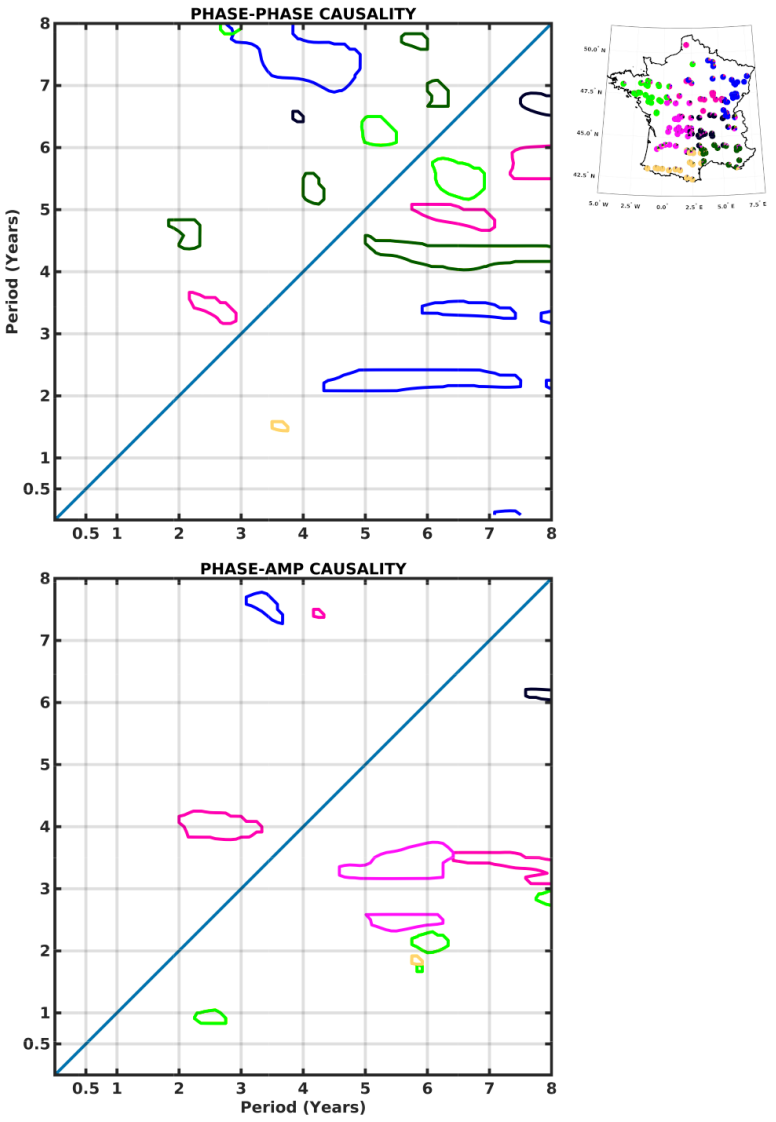

Figure S6. Precipitation cross-scale interactions (95% significance level).The driving time scale is on the horizontal axis, the driven on the vertical axis (*i.e.* the time scale x phase has a causal relationship with the phase/amplitude of the driven time scale y). Lower(upper) half of the graph, below (above) the diagonal, show time scales acting on smaller (larger) time scales. (**a**) Phase-phase causality. (**b**) Phase-amplitude causality.

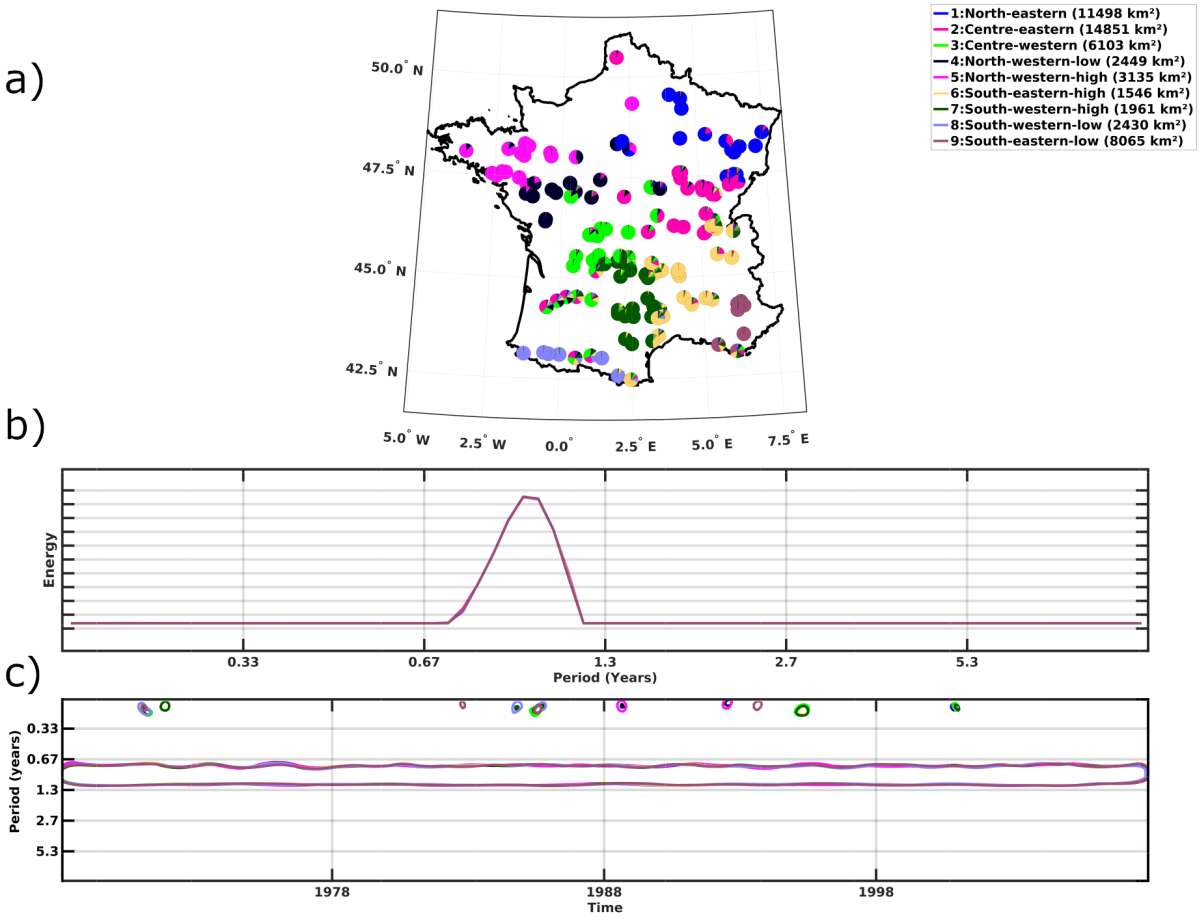

Figure S7. Clustering of temperature time-frequency variability in France. (**a**) Classification map of the watersheds. Pie charts slices show the three highest probability memberships (**b**) Global wavelet spectra for each cluster. (**c**) Statistically significant wavelet spectra for each cluster.

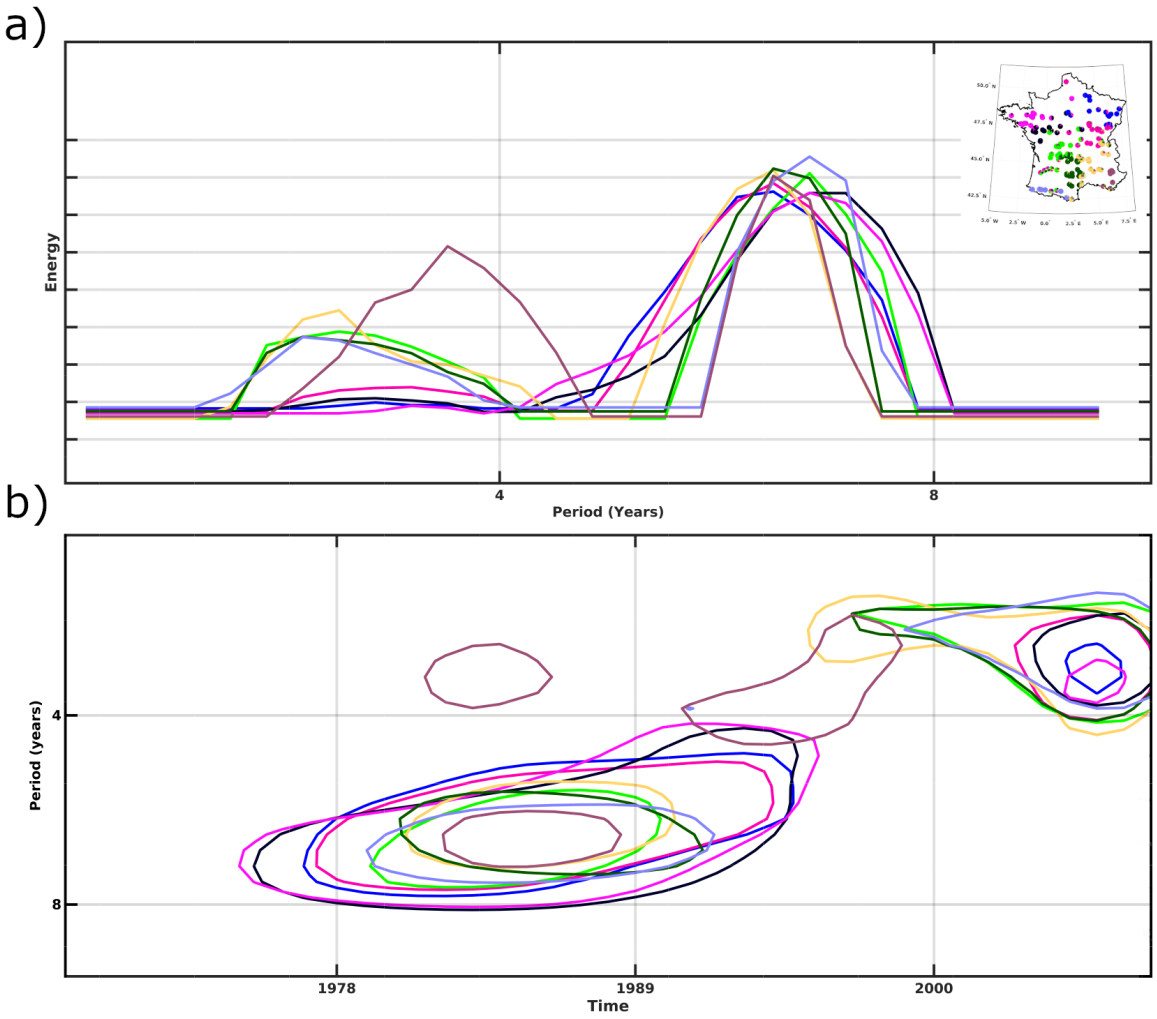

Figure S8. Inter-annual temperature time-frequency variability in France. (**a**) Global wavelet spectra for each cluster. (**b**) Statistically significant wavelet spectra for each cluster.

a)

b)

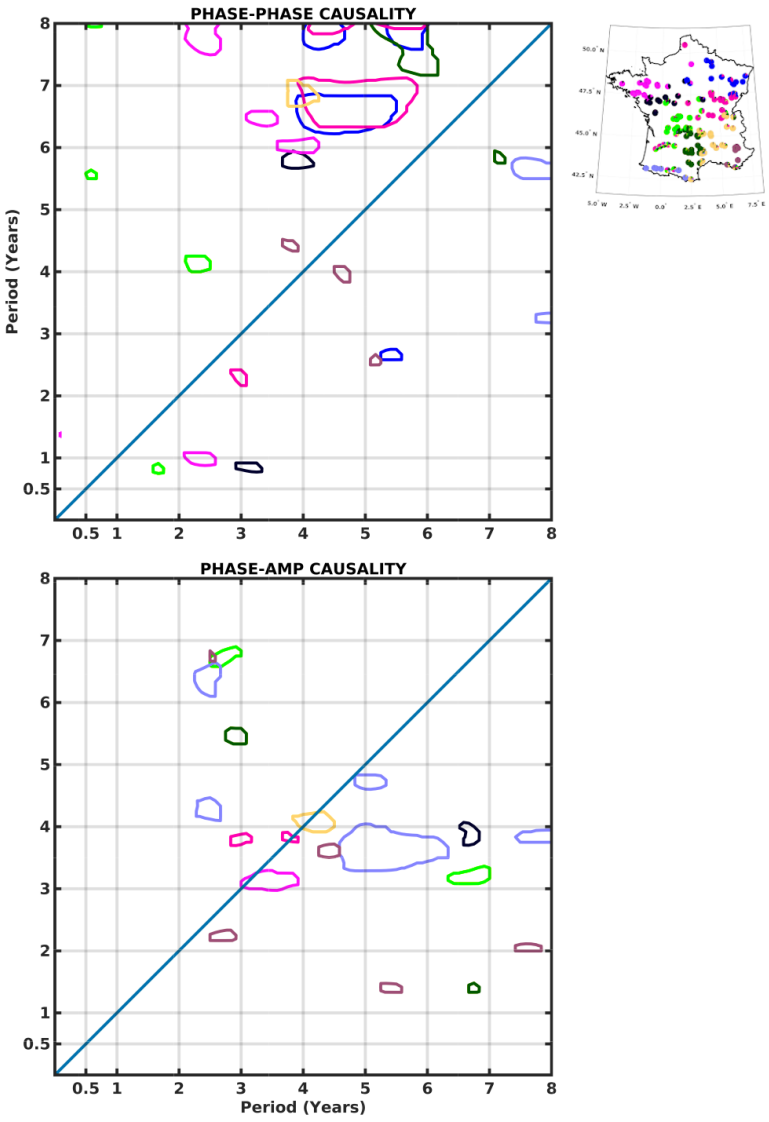

Figure S9. Temperature cross-scale interactions (95% significance level).The driving time scale is on the horizontal axis, the driven on the vertical axis (*i.e.* the time scale x phase has a causal relationship with the phase/amplitude of the driven time scale y). Lower(upper) half of the graph, below (above) the diagonal, show time scales acting on smaller (larger) time scales. (**a**) Phase-phase causality. (**b**) Phase-amplitude causality

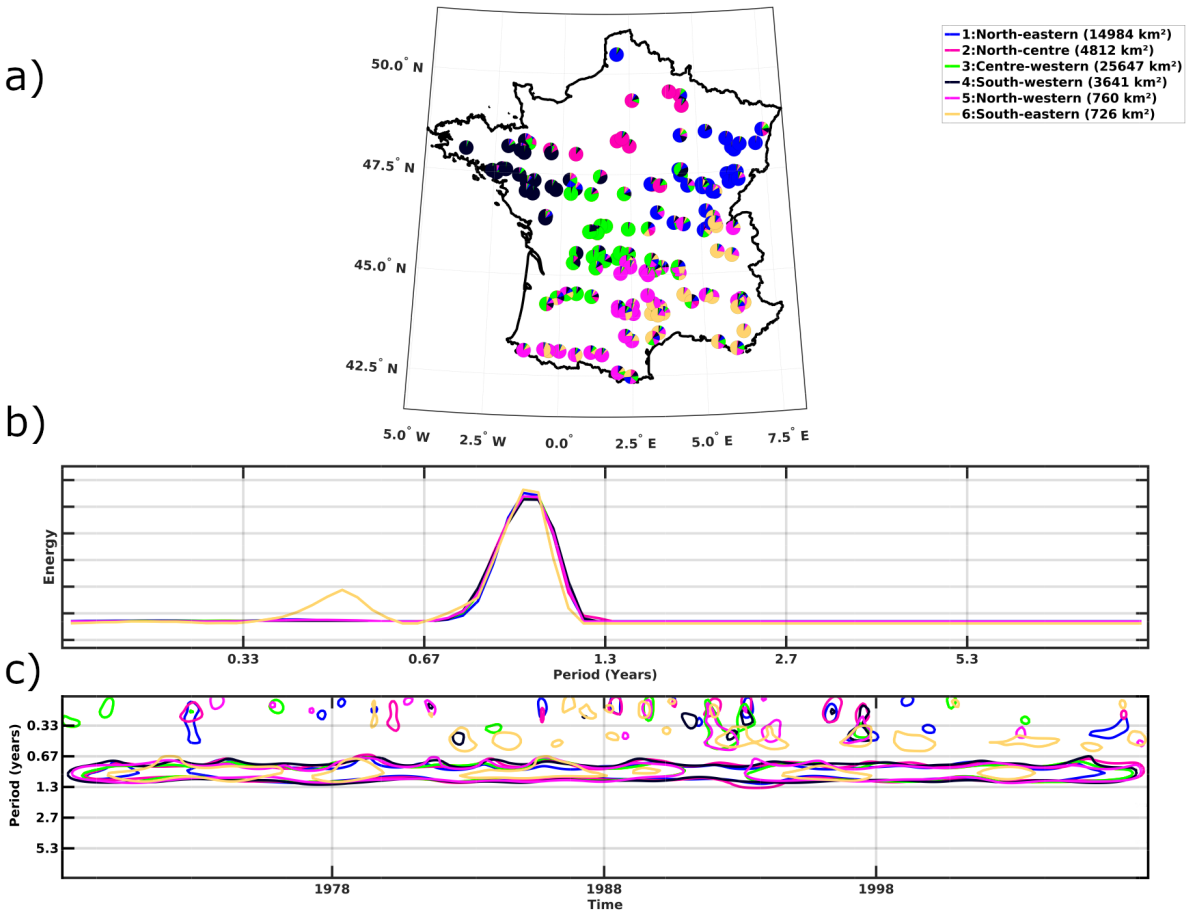

Figure S10. Clustering of discharge time-frequency variability in France. (**a**) Classification map of the watersheds. Pie charts slices show the three highest probability memberships (**b**) Global wavelet spectra for each cluster. (**c**) Statistically significant wavelet spectra for each cluster.

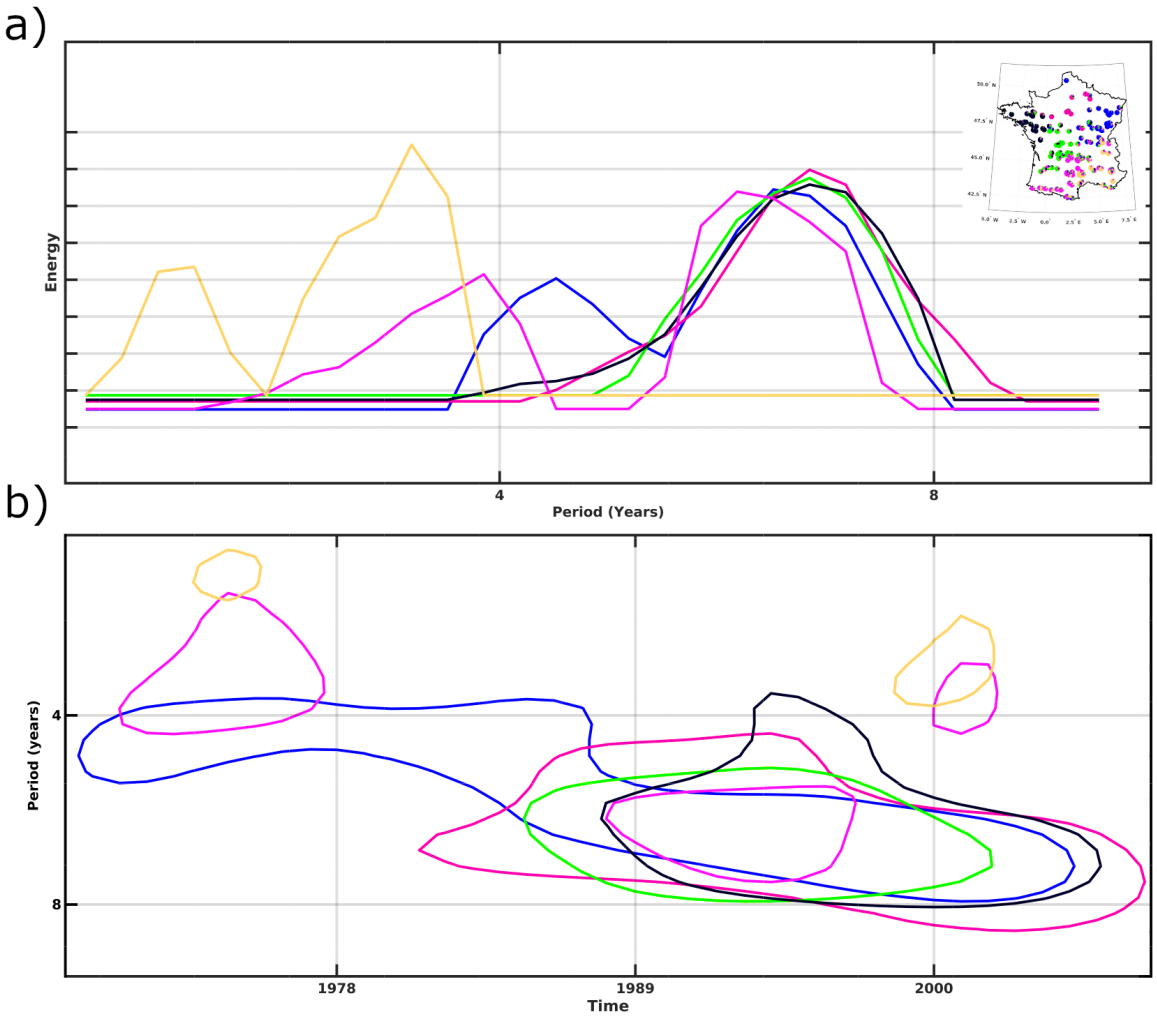

Figure S11. Inter-annual discharge time-frequency variability in France. (**a**) Global wavelet spectra for each cluster. (**b**) Statistically significant wavelet spectra for each cluster.

a)

b)

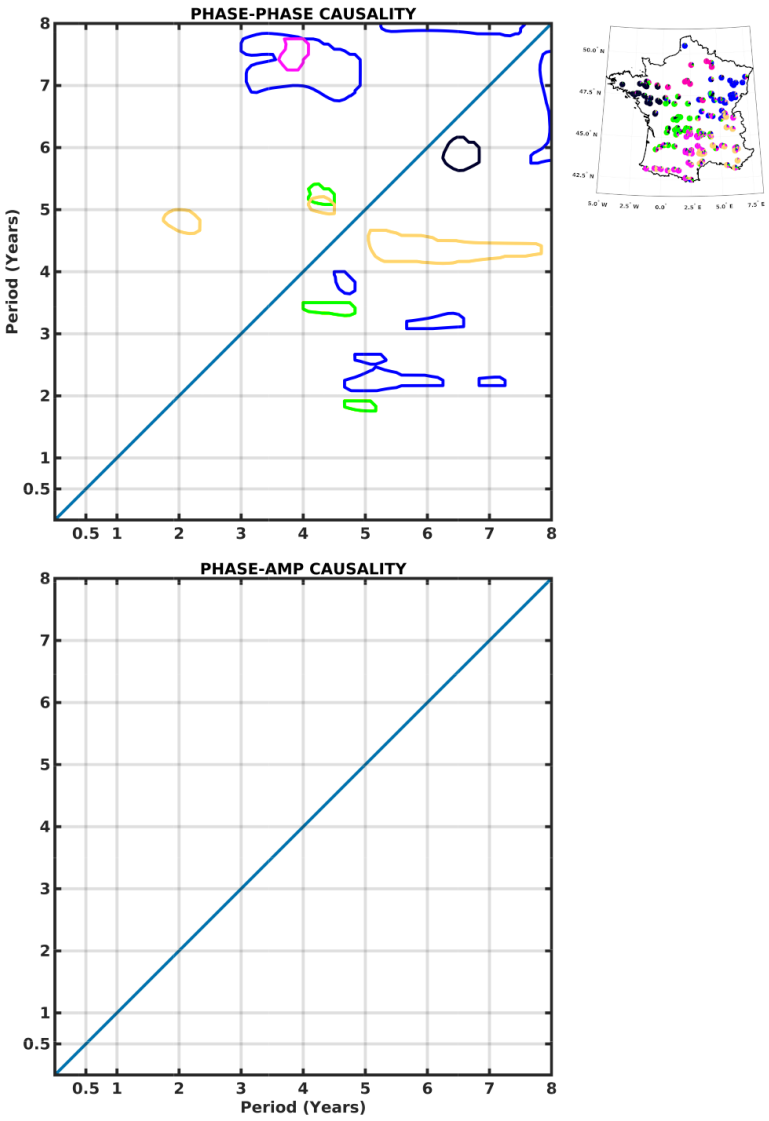

Figure S12. Discharge cross-scale interactions (95% significance level).The driving time scale is on the horizontal axis, the driven on the vertical axis (*i.e.* the time scale x phase has a causal relationship with the phase/amplitude of the driven time scale y). Lower(upper) half of the graph, below (above) the diagonal, show time scales acting on smaller (larger) time scales. (**a**) Phase-phase causality. (**b**) Phase-amplitude causality

References

Brigode, P., Génot, B., Lobligeois, F., and Delalgue, O.: Summary sheets of watershed-scale hydroclimatic observed data for France, https://doi.org/Summary sheets of watershed-scale hydroclimatic observed data for France, https://webgr.inrae.fr/activites/base-de-donnees/, 2020.

Onslow, A. C. E., Jones, M. W., and Bogacz, R.: A canonical circuit for generating phase-amplitude coupling, PLoS ONE, 9, https://doi.org/10.1371/journal.pone.0102591, 2014.

Pella, H., Lejot, J., Lamouroux, N., and Snelder, T.: The theoretical hydrographical network (RHT) for France and its environmental attributes, Geomorphologie: Relief, Processus, Environnement, 18, 317–336, https://doi.org/10.4000/geomorphologie.9933, 2012.

Vidal, J. P., Martin, E., Franchistéguy, L., Baillon, M., and Soubeyroux, J. M.: A 50-year high-resolution atmospheric reanalysis over France with the Safran system, International Journal of Climatology, 30, 1627–1644, https://doi.org/10.1002/joc.2003, 2010.